Research Article

Local Smoothness of Graph Signals

Miloš Daković [ID],[1] Ljubiša Stanković [ID],[1] and Ervin Sejdić[2]

[1]*University of Montenegro, Podgorica, Montenegro*
[2]*University of Pittsburgh, Pittsburgh, PA, USA*

Correspondence should be addressed to Miloš Daković; milos@ac.me

Analysis of vertex-varying spectral content of signals on graphs challenges the assumption of vertex invariance and requires the introduction of vertex-frequency representations as a new tool for graph signal analysis. Local smoothness, an important parameter of vertex-varying graph signals, is introduced and defined in this paper. Basic properties of this parameter are given. By using the local smoothness, an ideal vertex-frequency distribution is introduced. The local smoothness estimation is performed based on several forms of the vertex-frequency distributions, including the graph spectrogram, the graph Rihaczek distribution, and a vertex-frequency distribution with reduced interferences. The presented theory is illustrated through numerical examples.

1. Introduction

Graph signal processing is a new and quickly developing field. Many practical signals can be considered as graph signals. The theory and methods for processing the graph signals are introduced and presented in [1–5]. Graph signal processing applications in biomedical systems [6, 7] and analysis of big data [8] provide insight into the graph framework advantages and real-world potential.

In the case of large graphs, we may not be interested in the analysis of the entire graph signal, but rather interested in its local behavior. Signals with varying local vertex behaviors are a class of signals called nonstationary graph signals. One approach to the analysis of nonstationary graph signals is vertex-frequency analysis [7, 9–15], which is a counterpart of time-frequency analysis [16–18] in classic signal processing.

The main representatives of the vertex-frequency representations are local vertex spectrum and its energetic version, graph spectrogram. Window functions are used to localize graph signals in a neighborhood of the considered vertex [9, 12, 15].

Another important class of vertex-frequency representations, called the vertex-frequency energy distributions, were recently introduced in [13, 14]. This class is a counterpart to the class of quadratic time-frequency distributions in classic signal analysis. It has been shown that the graph version of the Rihaczek distribution is of special interest for graph

signals since it does not require a localization window. The reduced interference distributions can be derived from the Rihaczek distribution by using appropriate kernel functions. This class of representations, under certain conditions, satisfies marginal properties in both the vertex domain and the spectral domain.

An important concept that is used in classic time domain signal analysis for the description of local signal behavior around a time instant is the instantaneous frequency. The local smoothness is introduced in this paper as an extension of the instantaneous frequency concept to graph signal analysis. The local smoothness is defined by using the graph signal Laplacian matrix. The vertex-frequency representations can be highly concentrated along the local spectral index, corresponding to the local signal smoothness. This property is used to define local smoothness estimators based on the vertex-frequency representations.

After an introduction, we will review the fundamental theory of graph signal processing. This review will include the graph Fourier transform and the global signal smoothness in Section 2. Then, the local signal smoothness will be introduced and its properties derived within Section 3. The vertex-frequency representations, along with their connections to the local signal smoothness, will be presented in Section 4. The theory will be illustrated through a nonstationary graph signal example.

2. Graph Signals

A graph is defined as a set of vertices and a set of edges connecting these vertices. In signal processing, such a structure can be considered as the domain of a signal. The signal values are defined at the graph vertices. The graph Fourier transform (graph spectrum) is defined through the eigenvalue decomposition of the graph Laplacian matrix. Here, we will present a review of the graph spectrum and the global signal smoothness index calculated using the Laplacian matrix [10].

2.1. Graph Signal and Spectrum. A weighted undirected graph with N vertices will be considered. The edge weights w_{nm} are nonzero if there is an edge between the vertices n and m. If there is no edge between the vertices n and m, the corresponding weight is equal to zero, $w_{nm} = 0$. The weight matrix $\mathbf{W}$ is a matrix whose elements are w_{nm}. It is a symmetric matrix (since the underlying graph is undirected), with zeros on the main diagonal.

The definition of the graph Laplacian, using the weight matrix $\mathbf{W}$ and its elements w_{nm}, is given by

$$\mathbf{L} = \mathbf{D} - \mathbf{W}, \tag{1}$$

where $\mathbf{D}$ is a diagonal matrix, called the degree matrix. Its diagonal elements are obtained from w_{nm} as $d_{nn} = \sum_{m=1}^{N} w_{nm}$, while $d_{mn} = 0$ for $m \neq n$.

The Laplacian matrix, like any other quadratic matrix, can be written using its eigenvectors and eigenvalues as

$$\mathbf{L} = \mathbf{U}\mathbf{\Lambda}\mathbf{U}^T. \tag{2}$$

In this decomposition, the matrix $\mathbf{U}$ consists of the matrix $\mathbf{L}$ eigenvectors, denoted by $\mathbf{u}_k$, as its columns. The diagonal matrix of eigenvalues λ_k, $k = 1, 2, \ldots, N$, is denoted by $\mathbf{\Lambda}$. The eigenvectors and eigenvalues of $\mathbf{L}$ are calculated from $\mathbf{L}\mathbf{u}_k = \lambda_k \mathbf{u}_k$. Here we will consider the case with simple eigenvalues, whose multiplicity is one.

Graph signal samples, $x(n)$, $n = 1, 2, \ldots, N$, are sensed/defined at each graph vertex n. These signal samples can be written in vector form as an $N \times 1$ vector:

$$\mathbf{x} = [x(1), x(2), \ldots, x(N)]^T. \tag{3}$$

The graph discrete Fourier transform (GDFT) of a signal $\mathbf{x}$ is defined by [10]

$$\mathbf{X} = \text{GDFT}\{\mathbf{x}\} = \mathbf{U}^T\mathbf{x}. \tag{4}$$

The coefficients in the GDFT $\mathbf{X}$ are calculated as the projections of the considered graph signal to the eigenvectors

$$X(k) = \mathbf{u}_k^T \mathbf{x} = \sum_{n=1}^{N} x(n) u_k(n). \tag{5}$$

The inverse graph discrete Fourier transform (IGDFT) follows from the property $\mathbf{U}^T\mathbf{U} = \mathbf{I}$ that holds for the Laplacian matrix eigenvectors, where $\mathbf{I}$ is an identity matrix. The IGDFT relation is $\mathbf{x} = \mathbf{U}\mathbf{X}$, with

$$x(n) = \sum_{k=1}^{N} X(k) u_k(n). \tag{6}$$

The GDFT concept can be extended to the directed graphs. The cases of repeated eigenvalues can also easily be included in the analysis [19–21].

2.2. Global Graph Signal Smoothness. In classic signal analysis, when the signal domain is time, the signal $u(n)$ smoothness can be defined through a second-order difference $y(n) = -u(n-1) + 2u(n) - u(n+1)$. Since classic time domain signal processing can be considered as graph signal processing on a circular graph, the second-order difference can be written as $\mathbf{y} = \mathbf{L}\mathbf{u}$, where $\mathbf{L}$ is the Laplacian of the circular graph. The signal smoothness can be measured as cumulative energy of the signal changes $E_u = \sum_n (u(n) - u(n-1))^2$. It can also be calculated as $E_u = \sum_n u(n) y(n)$. In matrix notation, we get the quadratic form $E_u = \mathbf{u}^T\mathbf{L}\mathbf{u}$. This approach can be extended to general (non-circular) graphs.

From the Laplacian eigendecomposition, we have

$$\mathbf{L}\mathbf{u} = \lambda\mathbf{u} \tag{7}$$

or

$$\mathbf{u}^T\mathbf{L}\mathbf{u} = \lambda\mathbf{u}^T\mathbf{u} = \lambda = E_u, \tag{8}$$

since for an eigenvector $\mathbf{u}$ holds $\mathbf{u}^T\mathbf{u} = 1$. For an arbitrary eigenvector $\mathbf{u}_k$ and the corresponding eigenvalue λ_k, here we omitted index k for notation simplicity. The quadratic form of an eigenvector $\mathbf{u}$ is equal to the corresponding eigenvalue. This quadratic form can be used as a measure of the signal smoothness. We can write the quadratic form as

$$\mathbf{u}^T\mathbf{L}\mathbf{u} = \sum_{n=0}^{N-1} u(n) \sum_{m=0}^{N-1} w_{nm} (u(n) - u(m))$$
$$= \sum_{n=0}^{N-1} \sum_{m=0}^{N-1} w_{nm} \left(u^2(n) - u(n) u(m) \right). \tag{9}$$

Since $w_{nm} = w_{mn}$, the last relation can also be rewritten as

$$\mathbf{u}^T\mathbf{L}\mathbf{u} = \sum_{n=0}^{N-1} \sum_{m=0}^{N-1} w_{nm} \left(u^2(m) - u(n) u(m) \right). \tag{10}$$

The sum of the previous two relations produces

$$2\mathbf{u}^T\mathbf{L}\mathbf{u} = \sum_{n=0}^{N-1} \sum_{m=0}^{N-1} w_{nm} (u(n) - u(m))^2. \tag{11}$$

Obviously, a small value of $\mathbf{u}^T\mathbf{L}\mathbf{u} = \lambda$ corresponds to slow eigenvector variations $w_{nm}(u(n) - u(m))^2$, within the neighboring/connected vertices. This means that the eigenvectors calculated with a small λ represent a low-pass (slow-varying) part of the graph signal.

(a) Constant signal

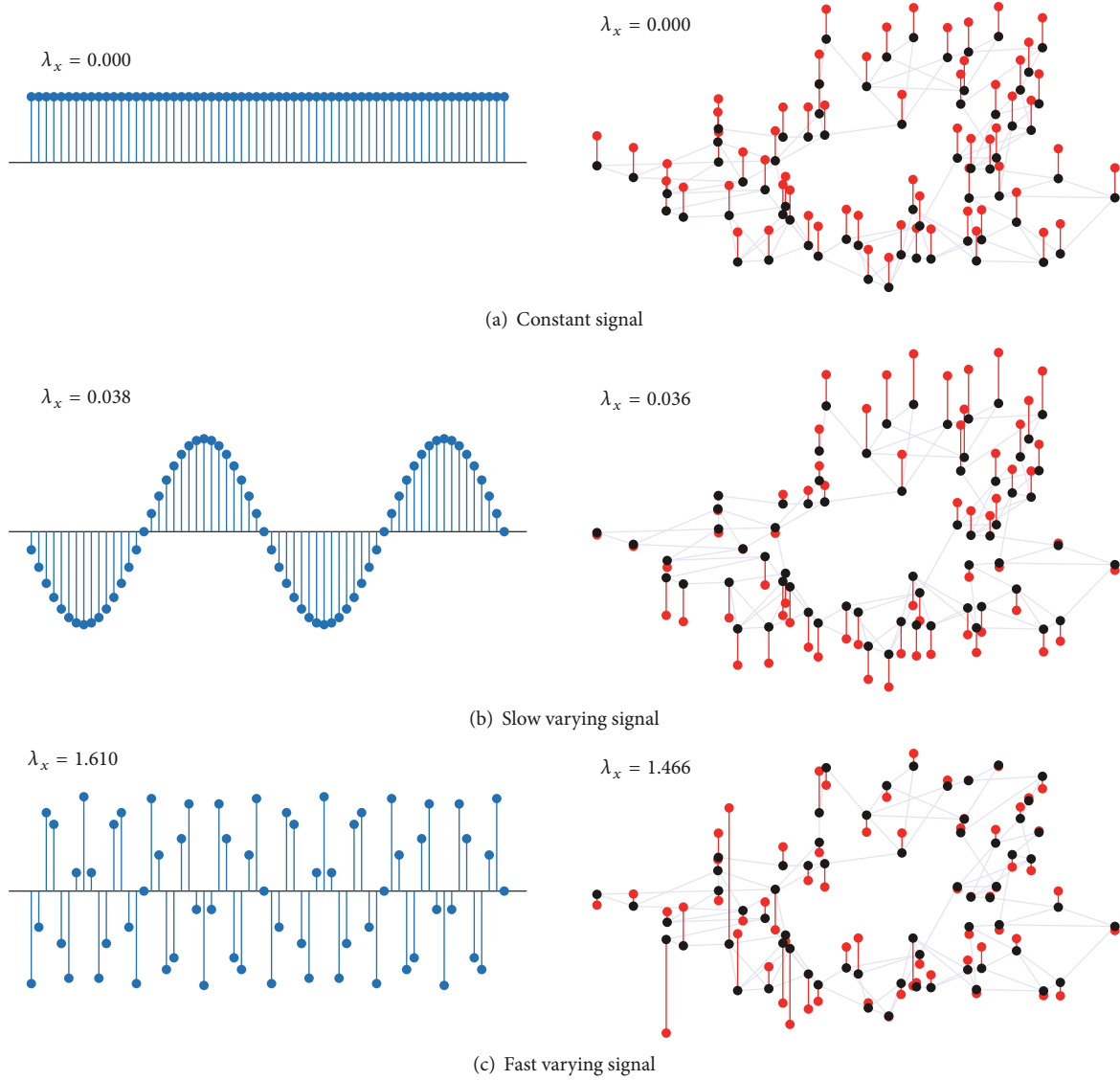

(b) Slow varying signal

(c) Fast varying signal

FIGURE 1: Signals in the time domain (left) and in the graph domain (right). The global signal smoothness λ_x is calculated and presented in the figure for each considered signal.

Since the eigenvalues of the Laplacian matrix are equal to the quadratic form $\mathbf{u}^T \mathbf{L} \mathbf{u}$, they are nonnegative. It is known that at least one eigenvalue of the Laplacian is zero. The corresponding eigenvector is constant, i.e., maximally smooth signal.

The graph signal $\mathbf{x}$ smoothness is defined, in general, using a full analogy with (8). By normalizing the quadratic form,

$$E_x = \mathbf{x}^T \mathbf{L} \mathbf{x}. \tag{12}$$

With the signal energy, the smoothness index λ_x definition is obtained as

$$\lambda_x = \frac{\mathbf{x}^T \mathbf{L} \mathbf{x}}{\mathbf{x}^T \mathbf{x}}. \tag{13}$$

An example of the time domain signals and graph signals, with various values of the global smoothness λ_x, is presented

in Figure 1. It is obvious that small λ_x values correspond to the smooth (slow-varying) signals and that large values of λ_x indicate fast-varying signals.

Now consider the signal whose form is given by a weighted sum of the eigenvectors,

$$x(n) = \sum_{i=1}^{M} x_i(n) = \sum_{i=1}^{M} \alpha_i u_{k_i}(n). \tag{14}$$

The global smoothness of this signal is

$$\lambda_x = \frac{\sum_{i=1}^{N} \alpha_i^2 \lambda_{k_i}}{\sum_{i=1}^{N} \alpha_i^2}. \tag{15}$$

It is obvious that $\lambda_{\min} \leq \lambda_x \leq \lambda_{\max}$, where $\lambda_{\min} = \min\{\lambda_{k_1}, \lambda_{k_2}, \ldots \lambda_{k_M}\}$ and $\lambda_{\max} = \max\{\lambda_{k_1}, \lambda_{k_2}, \ldots \lambda_{k_M}\}$.

The smoothness of graph signals is used in graph topology learning [22], vertex ordering, and graph clustering [23]. Since $\mathbf{u}_1$, corresponding to $\lambda_1 = 0$, is constant, the vertex ordering can be done using the next smoothest eigenvector $\mathbf{u}_2$ (called the Fiedler vector). The vertices are ordered according to the indices of the sorted $\mathbf{u}_2$ values. Regions with similar $\mathbf{u}_2$ values can be used for the graph clustering.

3. Local Graph Signal Smoothness

The local graph signal smoothness is introduced next. Its properties are analyzed in the second part of this section.

3.1. Local Graph Signal Smoothness Definition. Assume the simplest case, when the analyzed signal is proportional to the kth Laplacian eigenvector,

$$x(n) = \alpha u_k(n). \tag{16}$$

In a full analogy to classic spectral analysis, we can say that the signal of this form is a monocomponent signal, since its spectrum has only one nonzero coefficient at the kth position. We can define the spectral index of this component, or its smoothness index, as

$$\frac{\mathbf{x}^T \mathbf{L} \mathbf{x}}{\mathbf{x}^T \mathbf{x}} = \frac{\alpha^2 \mathbf{u}_k^T \mathbf{L} \mathbf{u}_k}{\alpha^2 \mathbf{u}_k^T \mathbf{u}_k} = \lambda_k. \tag{17}$$

It is equal to the corresponding eigenvalue.

The smoothness index can be related to the frequency in the time domain signal analysis [10]. The classic Fourier analysis may be obtained as a special case of the GDFT on a circular undirected graph. For this graph, the eigenvectors are periodic functions $u_k(n) = \cos(2\pi nk/N + \phi)$ with frequencies $\omega_k = 2\pi k/N$. The smoothness index is obtained from $\mathbf{L}\mathbf{u}_k = \lambda_k \mathbf{u}_k$ as

$$\lambda_k = 4 \sin^2\left(\frac{\omega_k}{2}\right) = \mathbf{u}_k^T \mathbf{L} \mathbf{u}_k. \tag{18}$$

We can conclude that the eigenvalue λ_k corresponds to the squared classic signal analysis frequency ω_k^2. If continuous-time is considered, instead of discrete-time, or the case with a small ω_k is considered in the discrete-time domain (18), we would get $\lambda_k \approx \omega_k^2$.

For the time domain signals with a time-varying spectrum, the concept of instantaneous frequency is introduced. Several approaches to the instantaneous frequency exist [16–18]. In general, for a signal with varying frequency, we can define instantaneous frequency by considering the signal behavior in the vicinity of the considered time instant t. If the signal form at the instant t and its small neighborhood is close to the form of a sinusoidal signal with frequency ω_t, then we can say that the instantaneous frequency of the considered signal, at the considered time instant t, is equal to $\omega(t)$. In this case, the frequency ω_t can be estimated by using a few samples around the considered time instant [24]. Another method to find the instantaneous frequency ω_t is to approximate the signal $x(t + \tau)$ by a second-order polynomial around $x(t)$,

$$x(t + \tau) \approx x(t) + x'(t)\tau + \frac{x''(t)\tau^2}{2}. \tag{19}$$

If we compare this signal with a sinusoidal signal expansion at the instant t, for a small τ,

$$\begin{aligned} A\cos\left(\omega_t(t+\tau) + \phi\right) &\approx A\cos\left(\omega_t t + \phi\right) \\ &\quad - A\omega_t \sin\left(\omega_t t + \phi\right)\tau \\ &\quad - \frac{A\omega_t^2 \cos\left(\omega_t t + \phi\right)\tau^2}{2}, \end{aligned} \tag{20}$$

we can conclude that, for $x(t) \neq 0$, the sinusoidal signal that fits the signal defined by (19), around the considered time instant t, has the frequency $\omega_t = \omega(t)$ such that

$$\omega_t^2 = \omega^2(t) = \lambda(t) = -\frac{x''(t)}{x(t)}. \tag{21}$$

Now we can conclude that the instantaneous frequency of the considered signal at a time instant t is $\omega(t)$. If $x(t) = 0$, we can use the ratio of higher-order derivatives $x^{(n+2)}(t)/x^{(n)}(t)$ in order to obtain the signal's instantaneous frequency (assuming that $x^{(n)}(t) \neq 0$).

The discrete-time definition of the squared instantaneous frequency is

$$\omega^2(n) = -\frac{x(n-1) - 2x(n) + x(n+1)}{x(n)} = \frac{\mathcal{L}_x(n)}{x(n)}, \tag{22}$$

where $\mathcal{L}_x(n) = -x(n-1) + 2x(n) - x(n+1)$ is the second-order difference of the considered signal.

In the previous section, we show that the second-order difference of a time domain signal corresponds to the elements of $\mathbf{L}\mathbf{x}$, where $\mathbf{L}$ is the Laplacian of a circular graph. An example of a signal with time-varying smoothness is presented in Figure 2. In the first part, $1 \leq n \leq 20$, the signal is slow-varying (with a small local smoothness), then a fast varying part of the signal follows, and in the last part, the signal is moderately smooth.

In analogy with (22), we will introduce the local smoothness for a signal defined on an arbitrary graph as

$$\lambda(n) = \frac{\mathcal{L}_x(n)}{x(n)}. \tag{23}$$

We have assumed that $x(n) \neq 0$.

3.2. Properties of the Local Smoothness. Some of the properties of the local smoothness are described next.

(1) Consider a monocomponent signal

$$x(n) = \alpha u_k(n). \tag{24}$$

Its local smoothness $\lambda(n)$ is vertex independent. This smoothness is equal to the global smoothness λ_k since

$$\mathcal{L}_x(n) = \alpha \mathcal{L}_{u_k}(n) = \alpha \lambda_k u_k(n). \tag{25}$$

In the time domain signal analysis, this property means that the instantaneous frequency of a sinusoidal signal is equal to its frequency.
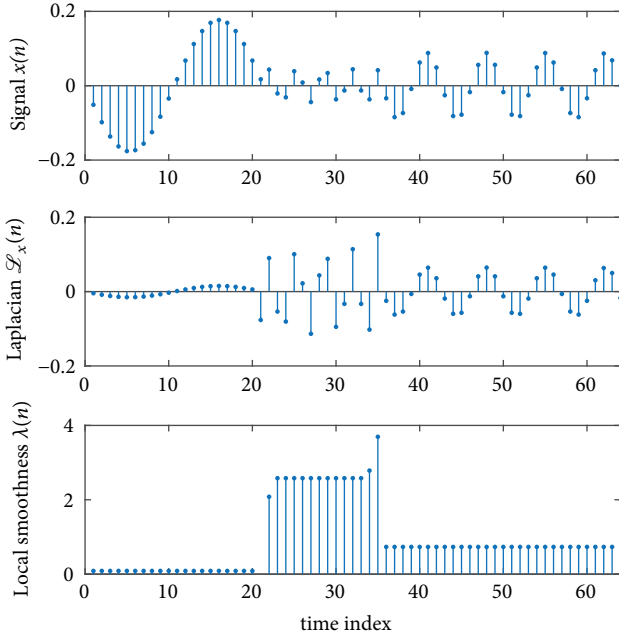
FIGURE 2: An example of the signal with varying local smoothness in the time domain.

(2) Assume a piecewise monocomponent signal

$$x(n) = \alpha_i u_{k_i}(n) \quad \text{for } n \in \mathscr{V}_i, \ i = 1, 2, \ldots, M, \quad (26)$$

where $\mathscr{V}_i$ are subsets of the vertices such that $\mathscr{V}_i \cap \mathscr{V}_j = \emptyset$ for $i \neq j$, and each vertex belongs to a subset $\mathscr{V}_i$. Within each subset, the considered signal is proportional to the eigenvector $u_{k_i}(n)$.

For each interior vertex $n \in \mathscr{V}_i$, i.e., a vertex whose neighborhood lies in the same set $\mathscr{V}_i$, the local smoothness is

$$\lambda(n) = \frac{\alpha_i \mathscr{L}_{u_{k_i}}(n)}{\alpha_i u_{k_i}(n)} = \lambda_{k_i}. \quad (27)$$

An example of a piecewise monocomponent graph signal is presented in Figure 3. Three subsets of vertices $\mathscr{V}_1$, $\mathscr{V}_2$, and $\mathscr{V}_3$ are considered. They are marked in colors in Figure 3. The component spectral indices are $k_1 = 54$, $k_2 = 38$, and $k_3 = 18$.

For subset $\mathscr{V}_1 = \{1, 2, \ldots, 22\}$, the boundary vertices are 1, 4, 6, 17, and 22. For subset $\mathscr{V}_2 = \{23, 24, \ldots, 34\}$, the boundary vertices are 23, 24, 29, and 34. For subset $\mathscr{V}_3 = \{35, 36, \ldots, 64\}$, the boundary vertices are 35, 39, 53, 62, and 64. All other vertices are interior vertices.

The local smoothness of the piecewise monocomponent graph signal from Figure 3 is calculated and presented in Figure 4. The obtained results are exact for each interior vertex (presented with dots in Figure 4). For the boundary vertices, the results are not exact since we include samples from all neighboring
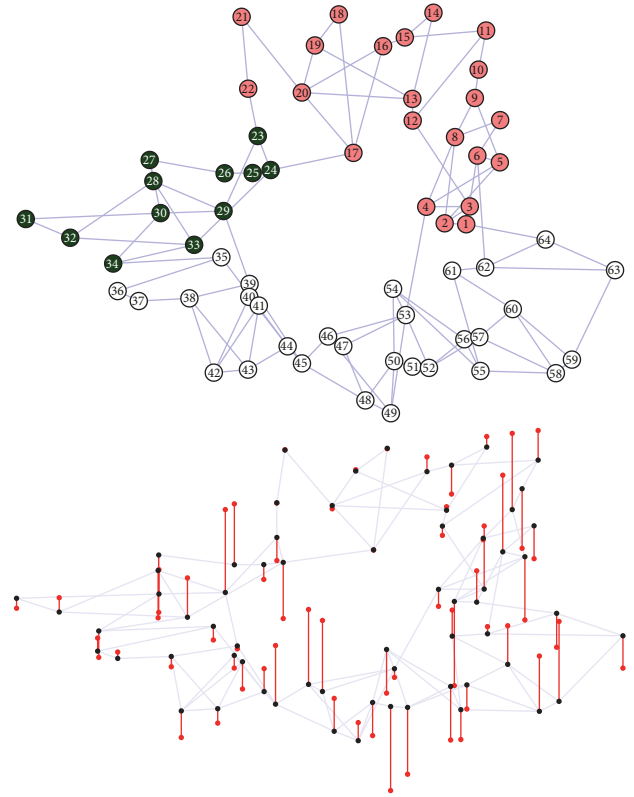

FIGURE 3: Piecewise monocomponent signal on the graph. The signal is composed of three parts. The support sets $\mathscr{V}_1$, $\mathscr{V}_2$, and $\mathscr{V}_3$ are presented with different vertex colors.
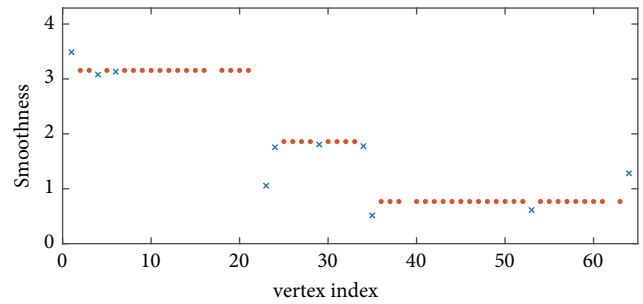

FIGURE 4: The local smoothness values for the graph signal shown in Figure 3. The local smoothness values at the interior vertices are indicated by the red dots. The local smoothness values at the boundary vertices are indicated by the blue cross marks.

vertices in the local smoothness calculation. Some of them are outside the considered set $\mathscr{V}_i$. The results for the boundary vertices are indicated by the cross marks.

(3) An ideal vertex-frequency distribution can be defined as

$$I(n, k) \sim |x(n)|^2 \delta(\lambda_k - \lambda(n)). \quad (28)$$

It has been assumed that the local smoothness is rounded to the nearest eigenvalue.
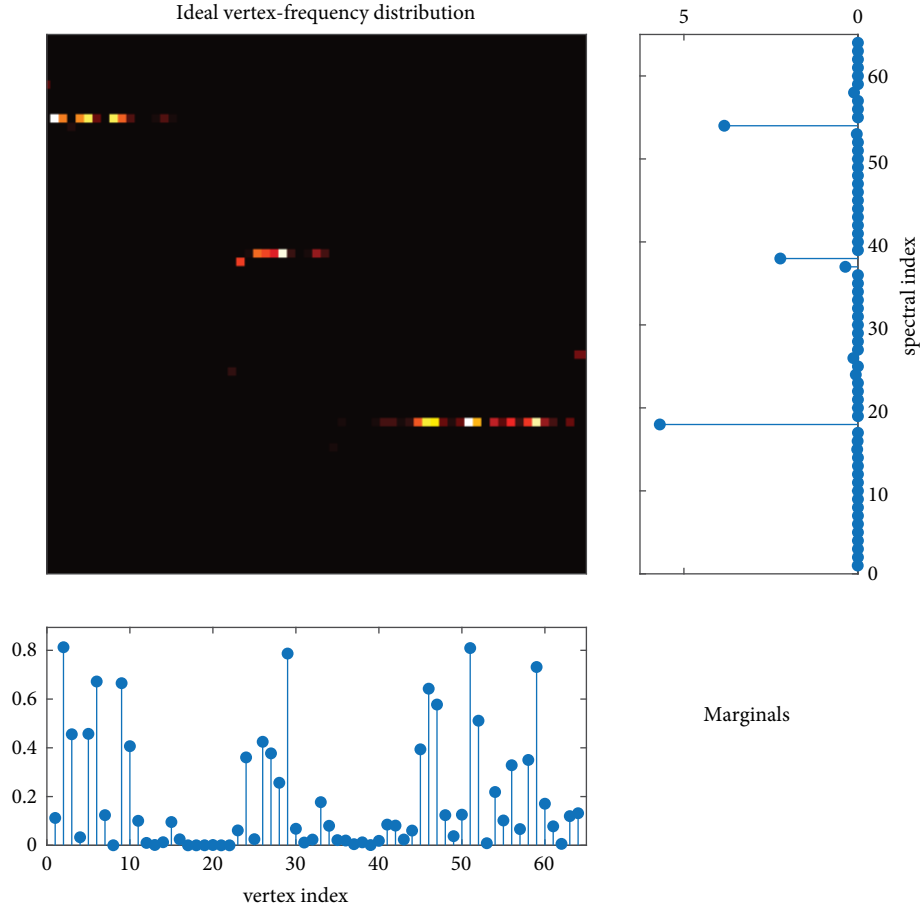
FIGURE 5: The ideal vertex-frequency distribution of a graph signal.

For the graph and the signal presented in Figure 3, the ideal vertex-frequency distribution is shown in Figure 5.

This distribution can be used as a local smoothness estimator since, for each vertex n, the maximum of $I(n, k)$ is positioned at $\lambda_k = \lambda(n)$. The index of the eigenvalue that corresponds to the local smoothness $\widehat{k}$ is obtained as

$$\widehat{k}(n) = \arg \max_k \{I(n, k)\}, \tag{29}$$

and the estimated local smoothness is $\widehat{\lambda}(n) = \lambda_{\widehat{k}(n)}$. This estimator is common and widely used in classic time-frequency analysis [16–18].

(4) For a multicomponent graph signal with M components,

$$x(n) = \sum_{i=1}^{M} x_i(n) = \sum_{i=1}^{M} \alpha_i u_{k_i}(n), \tag{30}$$

the local smoothness, calculated by definition, is

$$\lambda(n) = \frac{\sum_{i=1}^{M} \alpha_i \mathscr{L}_{u_{k_i}}(n)}{\sum_{i=1}^{M} \alpha_i u_{k_i}(n)} = \frac{\sum_{i=1}^{M} \alpha_i \lambda_{k_i} u_{k_i}(n)}{\sum_{i=1}^{M} \alpha_i u_{k_i}(n)}. \tag{31}$$

From classic time domain analysis, we know that a multicomponent signal cannot be analyzed directly; that is, the instantaneous frequency is not defined as a single value in this case. We can only estimate the instantaneous frequencies of the individual components. The same holds for graph signals, where we should decompose multicomponent signals to the individual components and then calculate the local smoothness for each component.

(5) A vertex-frequency distribution $G(n, k)$ satisfies the local smoothness property if

$$\frac{\sum_{k=1}^{N} \lambda_k G(n, k)}{\sum_{k=1}^{N} G(n, k)} = \lambda(n). \tag{32}$$

The ideal vertex-frequency distribution $I(n, k)$ satisfies the local smoothness property under the assumption that $\lambda(n) \in \{\lambda_1, \lambda_2, \ldots, \lambda_N\}$ for all n.

(6) For a vertex-frequency distribution $G(n, k)$ that satisfies the local smoothness property, the local smoothness bandwidth is defined by

$$\sigma_\lambda^2(n) = \frac{\sum_{k=1}^{N}(\lambda_k - \lambda(n))^2 G(n,k)}{\sum_{k=1}^{N} G(n,k)}$$

$$= \frac{\sum_{k=1}^{N} \lambda_k^2 G(n,k)}{\sum_{k=1}^{N} G(n,k)} - \lambda^2(n). \tag{33}$$

4. Vertex-Frequency Representations

The energy vertex-frequency distributions follow the concept of the time-frequency energy distributions in classic signal analysis. The estimation of the local smoothness can be obtained by using the vertex-frequency representations that localize the graph signal energy on the local smoothness. Here we will present the vertex-frequency energy distribution, a reduced interference vertex-frequency distribution, and the graph signal spectrogram, as the tools for local smoothness estimation.

4.1. Energy Vertex-Frequency Distributions. The energy of a signal $x(n)$ is commonly defined as

$$E = \sum_{n=1}^{N} x^2(n). \tag{34}$$

The signal $x(n)$ can be written as $x(n) = \sum_{k=1}^{N} X(k) u_k(n)$, where $X(k)$ is the GDFT of the signal. The signal energy is now

$$E = \sum_{n=1}^{N} \sum_{k=1}^{N} x(n)\left(X(k) u_k(n)\right) = \sum_{n=1}^{N} \sum_{k=1}^{N} E(n,k), \tag{35}$$

where the distribution of the signal energy in the vertex-frequency domain $E(n,k)$ is

$$E(n,k) = x(n) X(k) u_k(n)$$

$$= \sum_{m=1}^{N} x(n) x(m) u_k(m) u_k(n). \tag{36}$$

This distribution corresponds to the Rihaczek distribution in classic time-frequency analysis.

A vertex-frequency distribution $E(n,k)$ satisfies the marginal properties, if

$$\sum_{n=1}^{N} E(n,k) = |X(k)|^2$$

$$\sum_{k=1}^{N} E(n,k) = x^2(n). \tag{37}$$

The marginal properties state that the signal power $x^2(n)$ can be obtained by a summation of $E(n,k)$ over k and that the squared signal spectrum $|X(k)|^2$ can be obtained by a summation of $E(n,k)$ over n.

We will show that the vertex-frequency distribution defined by (36) satisfies the local smoothness property (32)

$$\frac{\sum_{k=1}^{N} \lambda_k E(n,k)}{\sum_{k=1}^{N} E(n,k)} = \frac{\sum_{k=1}^{N} \lambda_k x(n) X(k) u_k(n)}{\sum_{k=1}^{N} x(n) X(k) u_k(n)}$$

$$= \frac{x(n) \mathscr{L}_x(n)}{x^2(n)} = \frac{\mathscr{L}_x(n)}{x(n)} = \lambda(n), \tag{38}$$

since $\sum_{k=1}^{N} \lambda_k X(k) u_k(n) = \mathscr{L}_x(n)$ is the inverse GDFT of $\lambda_k X(k)$. In a matrix form, it is equal to

$$\mathbf{U}(\mathbf{\Lambda X}) = \mathbf{U\Lambda}\left(\mathbf{U}^T \mathbf{U}\right)\mathbf{X} = \left(\mathbf{U\Lambda U}^T\right)(\mathbf{UX}) = \mathbf{Lx}. \tag{39}$$

For the vertex-frequency distribution defined by (36), the local smoothness bandwidth (33) may be written in terms of $\mathbf{L}^2 \mathbf{x}$, $\mathbf{Lx}$, and $\mathbf{x}$, since $\sum_{k=1}^{N} \lambda_k^2 X(k) u_k(n)$ corresponds to the elements of $\mathbf{L}^2 \mathbf{x}$.

Example. The distribution $E(n,k)$ of the graph signal from Figure 3 is illustrated in Figure 6. The marginal properties (sums over n and over k) are presented below and right of the distribution image. Both marginal properties are satisfied, as expected. It is important to note that this distribution does not use a localization window. From the vertex-frequency representation, we can identify the signal components and the cross-terms. The cross-terms, well known in classic time-frequency analysis, are produced by mixing the signal components in the calculation of the distribution values $E(n,k)$. The third signal component of the signal analyzed in Figure 6 exists at vertices $n \in \mathcal{V}_1 = \{35, 36, \ldots, 64\}$ only, and the distribution $E(n,k)$ is nonzero for lower vertex indices n at $k_3 = 18$. Also, there is no signal component at $k = 27$, but $E(n, 27)$ is obviously not equal to zero.

4.2. Vertex-Frequency Distributions with Reduced Interference. In order to reduce the cross-terms interferences and to preserve the marginal properties, a general class of reduced interference time-frequency distributions is extended to the graph signals [14]. The frequency domain definition of the reduced interference energy distribution is

$$G(n,k)$$

$$= \sum_{p=1}^{N} \sum_{q=1}^{N} X(p) X^*(q) u_p(n) u_q^*(n) \phi(p,k,q), \tag{40}$$

where $\phi(p,k,q)$ is a kernel function. For $\phi(p,k,q) = \delta(q-k)$, the graph Rihaczek distribution (36) follows. The exponential kernel, a counterpart to the Choi-Williams kernel in classic time-frequency analysis, is defined as

$$\phi(p,k,q) = \frac{\exp\left(-\alpha\left(\left|\lambda_p - \lambda_k\right| / \left|\lambda_p - \lambda_q\right|\right)\right)}{s(q,p)}, \tag{41}$$

where

$$s(q,p) = \sum_{k=1}^{N} \exp\left(-\alpha \frac{\left|\lambda_p - \lambda_k\right|}{\left|\lambda_p - \lambda_q\right|}\right) \tag{42}$$

for $q \neq p$ and $\phi(p,k,p) = \delta(k-p)$.

Vertex-frequency energy distribution
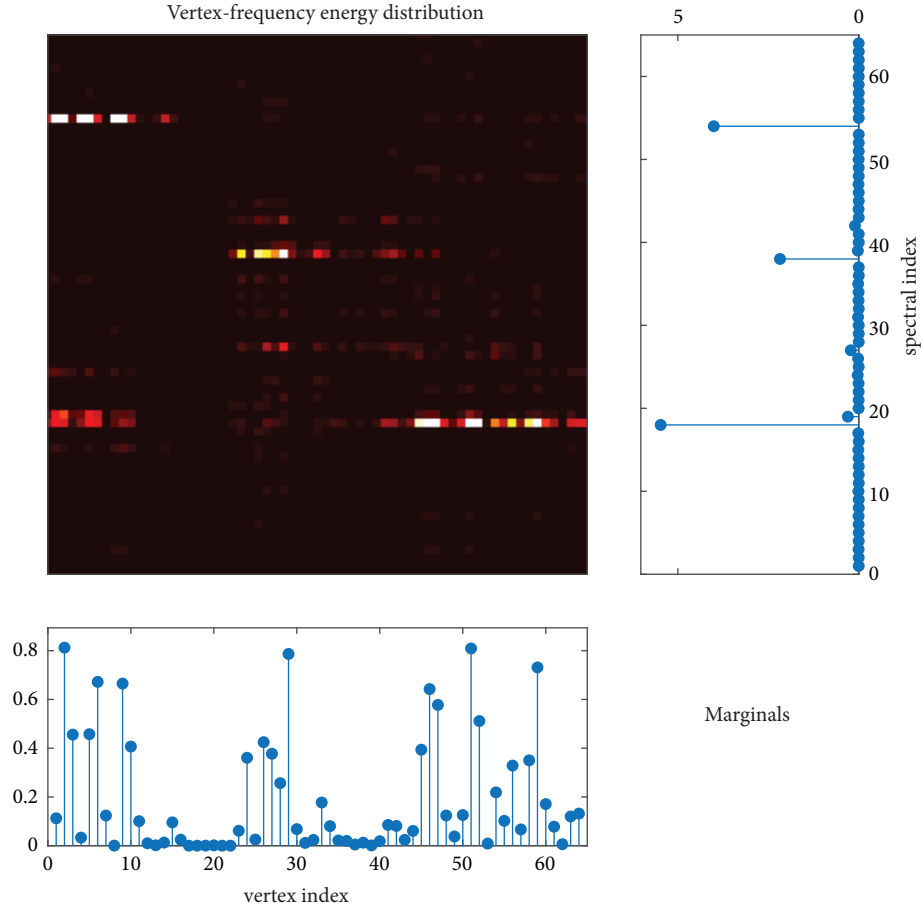

Marginals

FIGURE 6: Vertex-frequency energy distribution with its marginal values.

The reduced interference vertex-frequency distribution is presented in Figure 7. Here we have used the exponential kernel. It is notable that the cross-terms are reduced as compared to Figure 6, while the marginal properties are preserved in this case.

Now we will consider a general case and review the conditions that the distribution kernel should satisfy in order to preserve the marginal properties.

A sum of all $G(n, k)$ values should be equal to the signal energy

$$\sum_{k=1}^{N} \sum_{n=1}^{N} G(n, k) = E_x. \tag{43}$$

This relation is satisfied if

$$\sum_{k=1}^{N} \phi(p, k, p) = 1. \tag{44}$$

The vertex marginal property of the distribution $G(n, k)$ is satisfied if

$$\sum_{k=1}^{N} \phi(p, k, q) = 1 \tag{45}$$

since

$$\sum_{k=1}^{N} G(n, k) = \sum_{p=1}^{N} \sum_{q=1}^{N} X(p) X^*(q) u_p(n) u_q^*(n)$$
$$= |x(n)|^2. \tag{46}$$

Note that the eigenvectors are orthonormal, producing

$$\sum_{n=1}^{N} u_p(n) u_q^*(n) = \delta(p - q). \tag{47}$$

Moreover, if this condition is satisfied, then the vertex moment property holds

$$\sum_{n=1}^{N} \sum_{k=1}^{N} n^m G(n, k) = \sum_{n=1}^{N} n^m |x(n)|^2. \tag{48}$$

The frequency marginal property holds if

$$\phi(p, k, p) = \delta(p - k). \tag{49}$$

A sum of $G(n, k)$ over the vertex index k is

$$\sum_{n=1}^{N} G(n, k) = \sum_{p=1}^{N} |X(p)|^2 \phi(p, k, p) = |X(k)|^2. \tag{50}$$
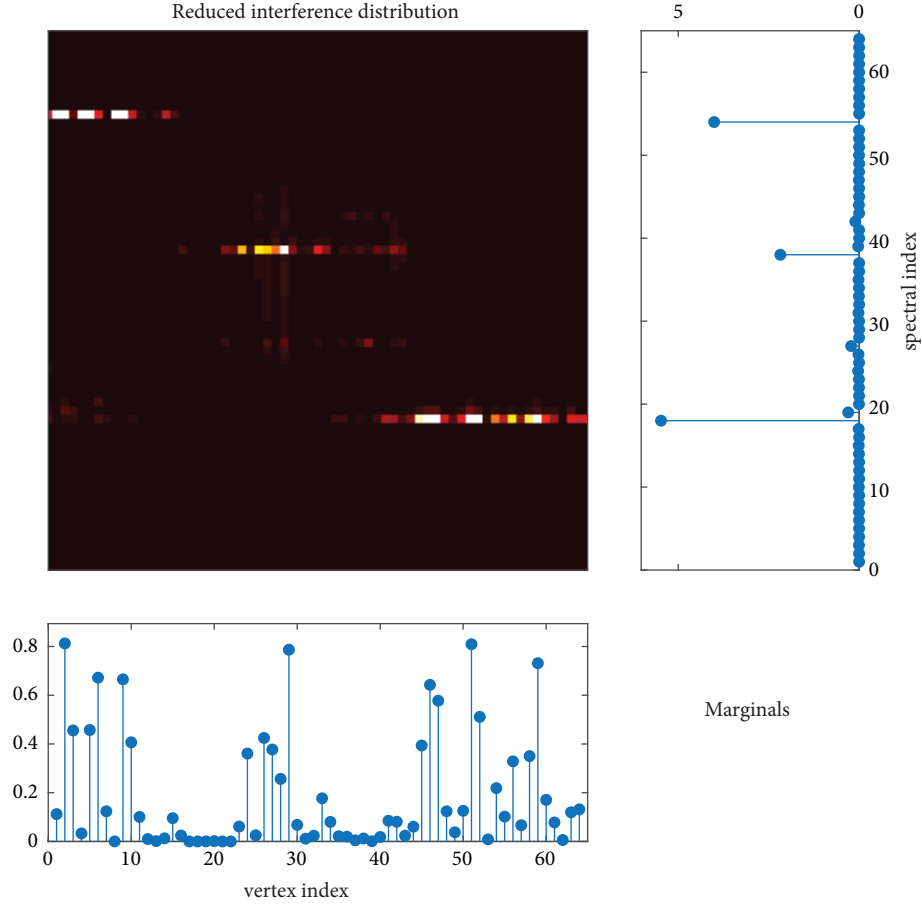
FIGURE 7: Reduced interference vertex-frequency distribution obtained using the exponential kernel.

If the frequency marginal property holds, then the frequency moment property holds as well,

$$\sum_{n=1}^{N} \sum_{k=1}^{N} k^m G(n,k) = \sum_{k=1}^{N} k^m |X(k)|^2 . \qquad (51)$$

The local smoothness property (32) of $G(n,k)$ is satisfied if

$$\frac{\sum_{k=1}^{N} \lambda_k G(n,k)}{\sum_{k=1}^{N} G(n,k)} = \frac{\mathcal{L}_x(n)}{x(n)} = \lambda(n). \qquad (52)$$

This can be written as

$$\frac{\sum_{k=1}^{N} \sum_{p=1}^{N} \sum_{q=1}^{N} X(p) X^*(q) u_p(n) u_q^*(n) \lambda_k \phi(p,k,q)}{\sum_{k=1}^{N} \sum_{p=1}^{N} \sum_{q=1}^{N} X(p) X^*(q) u_p(n) u_q^*(n) \phi(p,k,q)} \qquad (53)$$

$$= \lambda(n).$$

The local smoothness property is satisfied if

$$\sum_{k=1}^{N} \phi(p,k,q) = 1$$

$$\text{and } \sum_{k=1}^{N} \lambda_k \phi(p,k,q) = \lambda_p. \qquad (54)$$

The reduced interference distributions can be used as estimators of the local smoothness. The local smoothness is estimated as the eigenvalue that corresponds to the position of the maximum in $G(n,k)$, for a considered vertex n,

$$\widehat{\lambda}(n) = \lambda_{\widehat{k}(n)},$$

$$\widehat{k}(n) = \underset{k}{\operatorname{argmax}} \{G(n,k)\}. \qquad (55)$$

The reduced interference distribution $G(n,k)$, along with the marginal properties, is presented in Figure 7. Performance of the distribution as a local smoothness estimator will be illustrated through an example at the end of this section.

4.3. *Vertex-Frequency Spectrogram.* In the classic time-frequency analysis, the short-time Fourier transform and the spectrogram are well-developed tools for analysis of nonstationary signals. Their extension to the graph signals leads to the vertex-frequency spectrogram. It can be calculated as the spectrum of a signal $x(n)$ multiplied by an appropriate localization window function $h_m(n)$

$$S(m,k) = \sum_{n=1}^{N} x(n) h_m(n) u_k(n). \qquad (56)$$

The window function $h_m(n)$ should localize the signal content around the vertex m. In general, it is vertex-dependent, in contrast to the classic time domain spectrogram, where commonly the same window (with a shift in time) is used.

In a special case, when $h_m(n) = 1$, the localized vertex spectrum is equal to the standard spectrum $S(m,k) = X(k)$ for each m; that is, no vertex localization is performed. The second special case is a maximally localized window

$$h_m(n) = \begin{cases} 1 & \text{for } n = m \\ 0 & \text{for } n \neq m. \end{cases} \tag{57}$$

The localized vertex spectrum, in this case, is equal to the signal $S(m,k) = x(m)$, for each k, and we do not have any spectral resolution.

The spectrogram of a graph signal is defined as

$$|S(m,k)|^2 = \left| \sum_{n=1}^{N} x(n) h_m(n) u_k(n) \right|^2. \tag{58}$$

The vertex marginal of the spectrogram $|S(m,k)|^2$ is

$$\sum_{k=1}^{N} |S(m,k)|^2 = \sum_{k=1}^{N} S(m,k) \sum_{n=1}^{N} x(n) h_m(n) u_k(n)$$
$$= \sum_{n=1}^{N} |x(n) h_m(n)|^2, \tag{59}$$

where Parseval's theorem is used. It is obvious that the vertex marginal property is not satisfied for a general localization window $h_m(n)$. Only for a very specific case when $h_m(n) = \delta(n - m)$, the vertex marginal is equal to the signal energy $\sum_{n=1}^{N} |x(n) h_m(n)|^2 = x^2(m)$.

A summation over m and k should produce the total signal energy. For the vertex spectrogram, we get

$$\sum_{m=1}^{N} \sum_{k=1}^{N} |S(m,k)|^2 = \sum_{n=1}^{N} \left(|x(n)|^2 \sum_{m=1}^{N} |h_m(n)|^2 \right). \tag{60}$$

If the localization windows are such that $\sum_{m=1}^{N} |h_m(n)|^2 = 1$ holds for all n, then the vertex spectrogram $|S(m,k)|^2$ is energy unbiased

$$\sum_{m=1}^{N} \sum_{k=1}^{N} |S(m,k)|^2 = \sum_{n=1}^{N} |x(n)|^2 = E_x. \tag{61}$$

The localization windows $h_m(n)$ could be defined in the spectral domain using a generalized graph convolution [9] or in the vertex domain using the vertex neighborhood [12].

(i) The localization window, defined in the spectral domain, is equal to [9]

$$h_m(n) = \sum_{k=1}^{N} H(k) u_k(m) u_k(n), \tag{62}$$

where $H(k)$ is a window basic function defined in the spectral domain, for example, as

$$H(k) = C \exp(-\lambda_k \tau), \tag{63}$$

where C is the amplitude of the window and $\tau > 0$ is a constant that defines the width of the window. The vertex-frequency spectrogram calculated with localization windows defined in the spectral domain is presented in Figure 8. It is obvious that the marginal properties are not satisfied in this case.

(ii) The localization window $h_m(n)$ can be defined in the vertex domain. The window function value depends on the distance d_{mn} between the vertices m and n

$$h_m(n) = g(d_{mn}), \tag{64}$$

where $g(d)$ is a form of the basic window that corresponds to the classic signal processing window form.

Here we will review a method for obtaining the localization window functions, at each vertex, in matrix form [10]. The vertices whose distance is $d_{mn} = 1$ follow from matrix $\mathbf{A}_1$. This matrix is equal to the graph adjacency matrix. The matrix $\mathbf{A}$, with elements a_{mn}, is obtained from the weighting matrix $\mathbf{W}$

$$a_{mn} = \begin{cases} 1 & \text{for } w_{mn} > 0 \\ 0 & \text{for } w_{mn} = 0. \end{cases} \tag{65}$$

The vertices whose distance is $d_{mn} = 2$ follow from the matrix

$$\mathbf{A}_2 = (\mathbf{A} \odot \mathbf{A}_1) \circ (\mathbf{1} - \mathbf{A}_1) \circ (\mathbf{1} - \mathbf{I}). \tag{66}$$

We have used the following notation: $\odot$ for the logical (Boolean) matrix product, $\circ$ for the Hadamard product (element-by-element multiplication), and $\mathbf{1}$ for the matrix whose all elements are equal to 1. The elements $a_{mn}^{(2)}$ of the matrix $\mathbf{A}_2$ are equal to 1 if the distance between vertices m and n is 2, and 0 otherwise. Matrix $\mathbf{A} \odot \mathbf{A}_1$ gives the information about all vertices that are connected with walks of the length 2 and a lower walk. The element-by-element multiplication by the matrix $\mathbf{1} - \mathbf{A}_1$ removes the vertices connected with walks of length 1, while the multiplication by $\mathbf{1} - \mathbf{I}$ removes the diagonal elements.

When $d_{mn} = d \geq 2$, a recursive relation for the matrix follows. It will give the information about the vertices at a distance d

$$\mathbf{A}_d = (\mathbf{A} \odot \mathbf{A}_{d-1}) \circ (\mathbf{1} - \mathbf{A}_{d-1}) \circ (\mathbf{1} - \mathbf{I}). \tag{67}$$

The matrix for the graph localization windows is formed as

$$\mathbf{P}_D = g(0) \mathbf{I} + g(1) \mathbf{A}_1 + \cdots + g(D-1) \mathbf{A}_{D-1}. \tag{68}$$
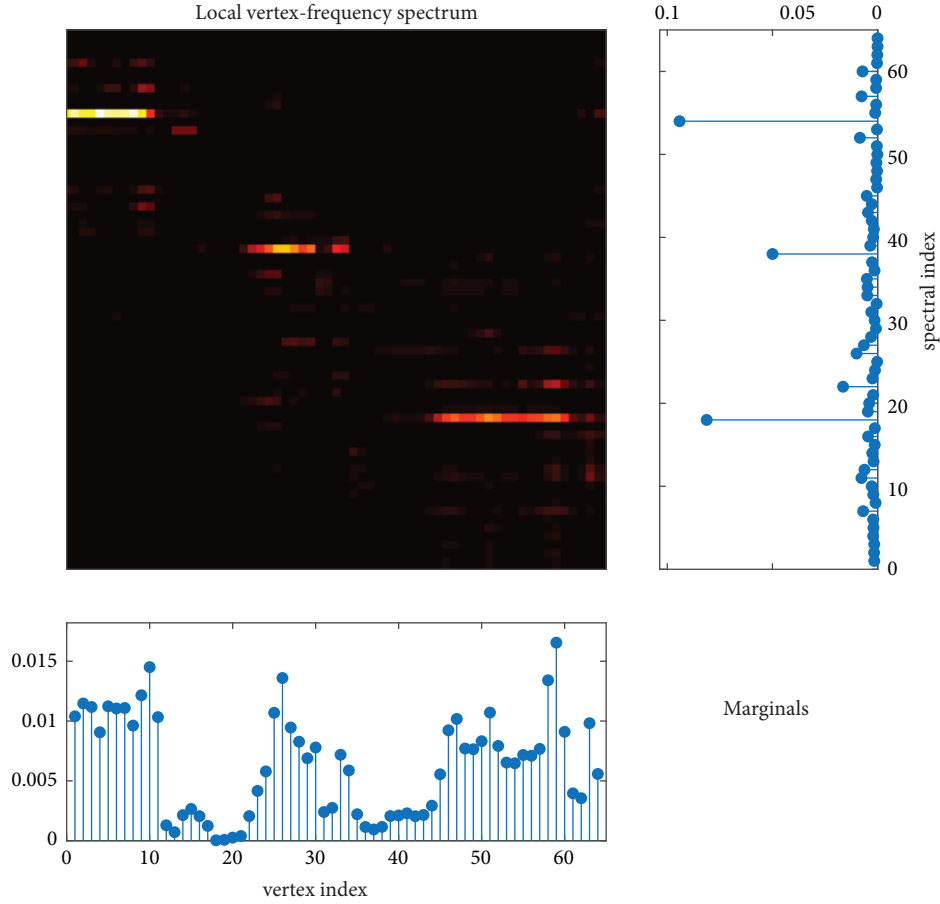
FIGURE 8: Local vertex-frequency spectrum calculated by using the localization windows defined in the spectral domain.

The graph signal weighted by the localization window is calculated by using the previous matrix as

$$x_m(n) = h_m(n)\, x(n) = P_D(n,m)\, x(n). \tag{69}$$

An example of the vertex-frequency spectrogram calculated by the vertex domain localization window is presented in Figure 9.

The relation that would connect the vertex domain spectrogram (56) and a general vertex-frequency distribution (40) is very complex. In order to establish this relation, the general vertex-frequency distribution should be rewritten using a kernel function in the vertex-vertex shift domain. This form is dual to (40)

$$G(n,k) = \sum_{m=1}^{N} \sum_{l=1}^{N} x(m)\, x^*(l)\, u_k(m)\, u_k^*(l)\, \varphi(m,n,l), \tag{70}$$

where $\varphi(m,n,l)$ is the vertex-vertex shift kernel. The conditions for the frequency marginal and the vertex marginal with a vertex-vertex shift kernel are

$$\sum_{n=1}^{N} \varphi(m,n,l) = 1 \tag{71}$$

$$\varphi(m,n,m) = \delta(m-n).$$

The kernel that corresponds to the vertex domain spectrogram (56) is

$$\varphi(m,n,l) = h_n(m)\, h_n^*(l). \tag{72}$$

For localization windows defined in the spectral domain, the kernel function can be written as

$$\varphi(m,n,l) = \sum_{p=1}^{N} \sum_{q=1}^{N} H(p)\, H^*(q)\, u_p(m)\, u_p(n)\, u_q^*(l)\, u_q^*(n). \tag{73}$$

This kernel cannot satisfy both marginal properties. The unbiased energy condition is

$$\sum_{n=1}^{N} \varphi(m,n,m) = 1. \tag{74}$$

Here, the local smoothness property cannot be satisfied. However, since the graph spectrogram is concentrated along the local smoothness, we can still use the maximum-based estimator of the local smoothness

$$\widehat{\lambda}(n) = \lambda_{\widehat{k}(n)},$$
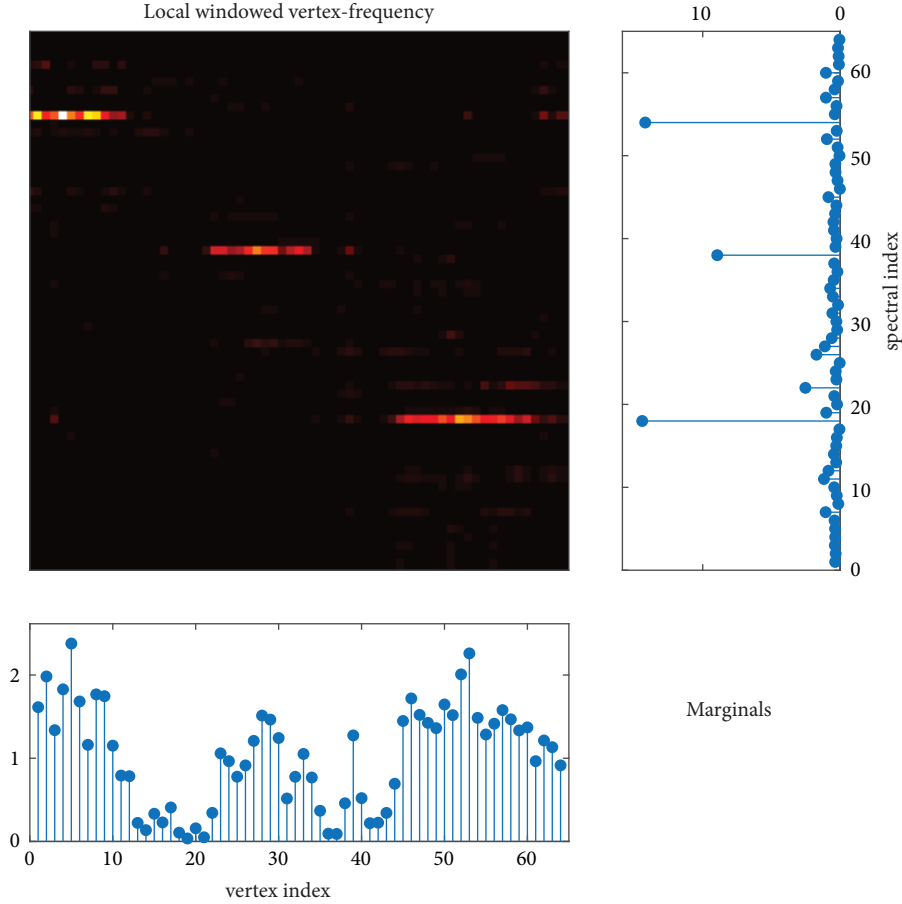$$\widehat{k}(n) = \arg\max_{k} \left\{ |S(n,k)|^2 \right\}. \tag{75}$$

Figure 9: Local vertex-frequency spectrum calculated using the vertex neighborhood windows.

5. Numerical Results

Now we will calculate the local signal smoothness by using the Laplacian applied to the graph signal (23) as well as the maximum positions of the Rihaczek distribution, the reduced interference distribution, and the local vertex spectrum with the spectral domain and the vertex domain windows. We will use the signal presented in Figure 3. The spectral domain window, defined by (62) and (63), is calculated with $C = 1$ and $\tau = 2$. The vertex domain window is calculated according to (68), with $D = 4$ and $g(d) = \cos^2(d\pi/8)$, i.e., $g(0) = 1$, $g(1) = 0.8536$, $g(2) = 0.5$, and $g(3) = 0.1464$.

The obtained results are presented in Figure 10 and in the first row of Table 1. For all considered estimators, the local smoothness is estimated at the vertices where significant signal sample values are detected, $|x(n)|^2 > 0.05 \max_n |x(n)|^2$. The theoretical value of the local smoothness is presented by a line and the estimated values are presented by dots. The number of outliers (indicated by NO in Table 1) is the number of vertices where the estimated smoothness is not equal to the theoretical one. The mean squared error (MSE) of the local smoothness estimations is also given in Table 1, for each considered case.

Next, we will consider a noisy signal. The signal is corrupted by a Gaussian noise added to the signal samples.

Table 1: The number of outliers and the mean squared error of the local smoothness for the considered estimators.

	Laplacian		Rih. dist.		RID		LVS spec.		LVS vert.	
SNR	NO	MSE	NO	MSE	NO	MSE	NO	MSE	NO	MSE
∞	4	0.027	0	0.000	0	0.000	4	0.161	4	0.161
50	4	0.027	0	0.000	0	0.000	4	0.161	4	0.161
40	8	0.027	0	0.000	0	0.000	4	0.161	5	0.165
30	20	0.032	0	0.000	0	0.000	4	0.161	5	0.165
20	32	0.057	0	0.000	0	0.000	4	0.161	5	0.165
10	36	0.261	0	0.000	1	0.027	4	0.172	5	0.036
5	38	0.848	3	0.177	1	0.027	4	0.172	5	0.042
0	38	1.557	5	0.290	3	0.095	6	0.278	6	0.270
-2.5	38	2.294	11	0.648	8	0.693	6	0.278	7	0.282
-5	38	2.194	14	1.127	16	1.814	9	0.581	9	0.555
-7.5	38	2.701	21	2.115	19	2.293	11	0.667	12	0.826
-10	38	3.052	25	2.486	23	2.474	19	1.089	15	1.177
-15	38	3.469	33	3.005	33	3.477	27	1.683	27	2.503

Signal-to-noise ratio (SNR) is varied from −15db to 50dB. The number of outliers and the MSE are given in Table 1. We can conclude that the direct method of local smoothness
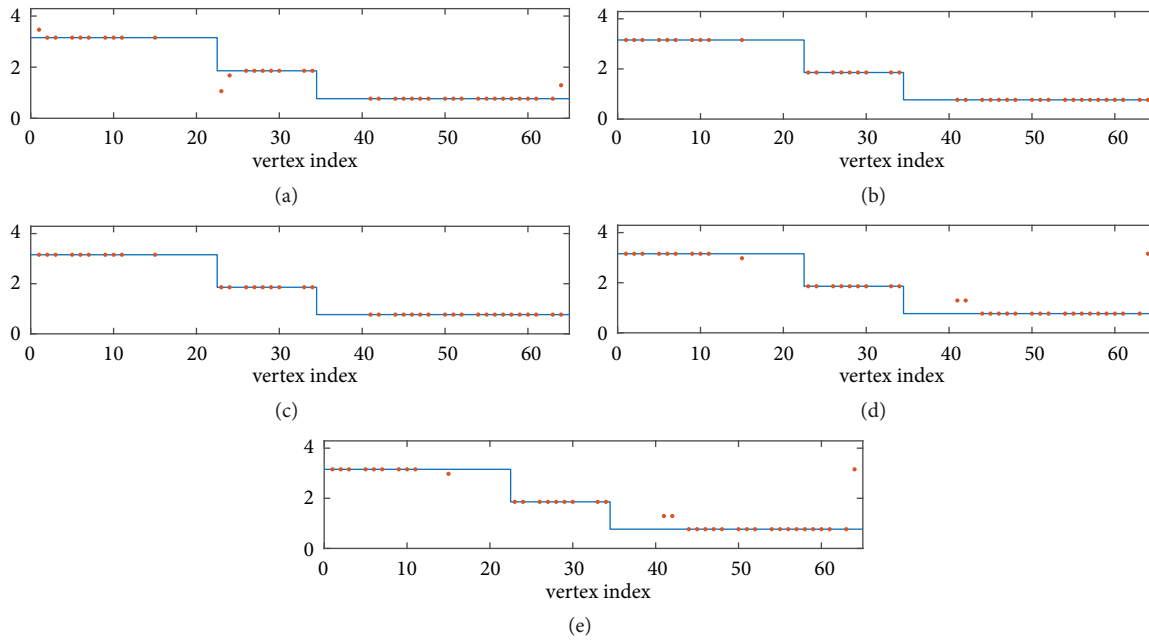
FIGURE 10: Local signal smoothness for the graph signal presented in Figure 3. Exact smoothness is presented by a solid line. The estimated smoothness is presented by dots. It is calculated only at the vertices where the signal takes significant values, $|x(n)|^2 > 0.05 \max_n |x(n)|^2$ using (a) the Laplacian of the graph signal (23), (b) the vertex-frequency energy distribution (Figure 6), (c) the reduced interference vertex-frequency distribution (Figure 7), (d) the graph spectrogram with a window defined in the vertex domain (Figure 9), and (e) the graph spectrogram with a window defined in the spectral domain (Figure 8).

estimation using the Laplacian is very sensitive to the noise, while the vertex-frequency based estimations are robust to the noise. For the local vertex spectrum, the number of outliers is slightly increased for the high SNR cases. This increase is caused by the signal smoothing. Note that the Rihaczek distribution and the reduced interference distribution provide better estimation for a high SNR, while for the SNR below 0dB, the local vertex spectrum, calculated with either the spectral or the vertex domain window, results in fewer outliers and a lower MSE.

The ratio of the concentration measures is calculated using the ℓ_1-norm of the Rihaczek distribution and the ℓ_1-norm of the reduced interference distributions [25]. It varied from 1.32 in the non-noisy case to 1.59 for the highest noise level.

6. Conclusion

In this paper, the local smoothness of graph signals is introduced and analyzed. Methods for local smoothness estimation, based on the signal Laplacian and the vertex-frequency representations, are given and applied to examples with graph signals. It has been shown that the local smoothness is a counterpart of the instantaneous frequency in classic signal analysis and can be estimated using vertex-frequency distributions. Finally, the vertex-frequency energy distributions, including a reduced interference distribution, and the local vertex spectrogram with two windowing techniques, are considered as the local smoothness estimators.

Data Availability

The data used to support the findings of this study are available from the corresponding author upon request.

Conflicts of Interest

The authors declare that they have no conflicts of interest.

References

[1] S. Chen, R. Varma, A. Sandryhaila, and J. Kovać, "Discrete signal processing on graphs: sampling theory," *IEEE Transactions on Signal Processing*, vol. 63, no. 24, pp. 6510–6523, 2015.

[2] A. Sandryhaila and J. M. Moura, "Discrete signal processing on graphs," *IEEE Transactions on Signal Processing*, vol. 61, no. 7, pp. 1644–1656, 2013.

[3] L. Stanković, M. Daković, and E. Sejdić, "Introduction to graph signal processing," in *Vertex-Frequency Analysis of Graph Signals*, pp. 3–108, Springer Nature, Cham, Swizerland, 2019.

[4] A. Sandryhaila and J. M. Moura, "Discrete signal processing on graphs: frequency analysis," *IEEE Transactions on Signal Processing*, vol. 62, no. 12, pp. 3042–3054, 2014.

[5] D. I. Shuman, S. K. Narang, P. Frossard, A. Ortega, and P. Vandergheynst, "The emerging field of signal processing on graphs: Extending high-dimensional data analysis to networks and other irregular domains," *IEEE Signal Processing Magazine*, vol. 30, no. 3, pp. 83–98, 2013.

[6] I. Jestrović, J. L. Coyle, and E. Sejdić, "Differences in brain networks during consecutive swallows detected using an optimized

vertex–frequency algorithm," *Neuroscience*, vol. 344, pp. 113–123, 2017.

[7] I. Jestrović, J. L. Coyle, and E. Sejdić, "A fast algorithm for vertex-frequency representations of signals on graphs," *Signal Processing*, vol. 131, pp. 483–491, 2017.

[8] A. Sandryhaila and J. M. F. Moura, "Big data analysis with signal processing on graphs: representation and processing of massive data sets with irregular structure," *IEEE Signal Processing Magazine*, vol. 31, no. 5, pp. 80–90, 2014.

[9] D. I. Shuman, B. Ricaud, and P. Vandergheynst, "Vertex-frequency analysis on graphs," *Applied and Computational Harmonic Analysis* , vol. 40, no. 2, pp. 260–291, 2016.

[10] L. Stankovi and E. Sejdi, "Vertex-frequency analysis of graph signals," *Springer Nature*, 2019.

[11] L. Stanković, M. Daković, and E. Sejdić, "Vertex-frequency energy distributions," in *Vertex-Frequency Analysis of Graph Signals*, pp. 377–415, Springer International Publishing, Cham, Swizerland, 2019.

[12] L. Stankovic, M. Dakovic, and E. Sejdic, "Vertex-frequency analysis: a way to localize graph spectral components," *IEEE Signal Processing Magazine*, vol. 34, no. 4, pp. 176–182, 2017.

[13] L. Stankovic, E. Sejdic, and M. Dakovic, "Vertex-frequency energy distributions," *IEEE Signal Processing Letters*, vol. 25, no. 3, pp. 358–362, 2018.

[14] L. Stankovic, E. Sejdic, and M. Dakovic, "Reduced interference vertex-frequency distributions," *IEEE Signal Processing Letters*, vol. 25, no. 9, pp. 1393–1397, 2018.

[15] D. I. Shuman, B. Ricaud, and P. Vandergheynst, "A windowed graph Fourier transform," in *Proceedings of the 2012 IEEE Statistical Signal Processing Workshop, SSP 2012*, pp. 133–136, USA, August 2012.

[16] L. Cohen, *Time-Frequency Analysis*, Prentice Hall PTR, 1995.

[17] B. Boashash, Ed., *Time-Frequency Signal Analysis and Processing, A Comprehensive Reference*, Academic Press, 2015.

[18] L. Stankovic', M. Dakovic', and T. Thayaparan, *Time-Frequency Signal Analysis with Applications*, Artech House, Boston, Mass, USA, March 2013.

[19] S. Sardellitti, S. Barbarossa, and P. D. Lorenzo, "On the graph fourier transform for directed graphs," *IEEE Journal of Selected Topics in Signal Processing*, vol. 11, no. 6, pp. 796–811, 2017.

[20] J. A. Deri and J. M. F. Moura, "Spectral projector-based graph fourier transforms," *IEEE Journal of Selected Topics in Signal Processing*, vol. 11, no. 6, pp. 785–795, 2017.

[21] R. Shafipour, A. Khodabakhsh, G. Mateos, and E. Nikolova, "A digraph fourier transform with spread frequency components," in *Proceedings of the 5th IEEE Global Conference on Signal and Information Processing (GlobalSIP)*, pp. 583–587, Montreal, QC, Canada, November 2017.

[22] X. Dong, D. Thanou, P. Frossard, and P. Vandergheynst, "Learning laplacian matrix in smooth graph signal representations," *IEEE Transactions on Signal Processing*, vol. 64, no. 23, pp. 6160–6173, 2016.

[23] D. Mejia, O. Ruiz-Salguero, and C. A. Cadavid, "Spectral-based mesh segmentation," *International Journal on Interactive Design and Manufacturing (IJIDeM)*, vol. 11, no. 3, pp. 503–514, 2017.

[24] T. Thayaparan, L. J. Stankovic', M. Dakovic', and V. Popovic'-Bugarin, "Micro-Doppler parameter estimation from a fraction of the period," *IET Signal Processing*, vol. 4, no. 3, pp. 201–212, June 2010.

[25] L. Stanković, "Measure of some time-frequency distributions concentration," *Signal Processing*, vol. 81, no. 3, pp. 621–631, 2001.

Advances in
Operations Research

Advances in
Decision Sciences

Journal of
Applied Mathematics

The Scientific World Journal

Journal of
Probability and Statistics

International
Journal of
Mathematics and
Mathematical
Sciences

Journal of
Optimization

International Journal of
Engineering
Mathematics

International Journal of
Analysis

Hindawi

Submit your manuscripts at
www.hindawi.com

Journal of
Complex Analysis

Advances in
Numerical Analysis

Mathematical Problems
in Engineering

International Journal of
Differential Equations

Discrete Dynamics in
Nature and Society

International Journal of
Stochastic Analysis

Journal of
Mathematics

Journal of
Function Spaces

Abstract and
Applied Analysis

Advances in
Mathematical Physics